

Non-cytotoxic and non-genotoxic wear debris of strontium oxide doped (Zirconia Toughened Alumina) (SrO-ZTA) implant for hip prosthesis

Nibedita Nayak^a, Shaik Akbar Basha^b, Surya Kant Tripathi^c, Bijesh K. Biswal^c,
Monalisa Mishra^{a,d,**}, Debasish Sarkar^{b,d,*}

^a Laboratory of Neural Developmental Biology, Department of Life Science, National Institute of Technology Rourkela, Odisha, 769008, India

^b Laboratory for Material Processing and Engineering, Department of Ceramic Engineering, National Institute of Technology, Rourkela, India

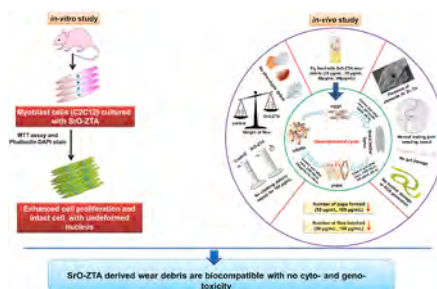
^c Laboratory of Cancer Drug Resistance, Department of Life Science, National Institute of Technology Rourkela, Odisha, 769008, India

^d Centre for Nanomaterials, National Institute of Technology, Rourkela, India

HIGHLIGHTS

- SrO-ZTA is non-cytotoxic and promotes growth of C2C12 mouse myoblast cells.
- Oral intake of SrO-ZTA nanocomposite has no toxic effect on the fly behaviour.
- No nuclear damage and oxidative stress level were observed in *D. melanogaster*.
- *In vitro* and *in vivo* studies validate SrO-ZTA as a non-toxic biocomposite.

GRAPHICAL ABSTRACT



ARTICLE INFO

Keywords:
Hip-implant
SrO-ZTA wear debris
C2C12 myoblast cells
Drosophila melanogaster
Toxicity

ABSTRACT

Bioceramic materials based biological implants have gained enormous attention in research due to their extensive medical application. However, release of wear debris from them limits their clinical relevance due to many health risks in the recipient. Thus, we decided to evaluate the cytotoxicity and genotoxicity of wear debris released from Strontium oxide doped Zirconia Toughened Alumina (SrO-ZTA) hip prosthesis developed in our laboratory. An extensive cytotoxicity analysis confirms that the cellular and nuclear morphology of C2C12 mouse myoblast cells are intact even after 72 h of SrO-ZTA wear debris exposure. Furthermore, treatment of wear debris in *Drosophila* model did not cause any damage to the larval gut epithelium and nuclei. Despite the reactive oxygen species (ROS) increase in third instar larvae after wear debris treatment at higher concentrations (50–100 µg/mL), the flies show appreciable weight gain, suggesting no harm to larva and flies. Interestingly, the eye, wing, and bristles of the hatched flies of all the experimental groups do not show any phenotypic defects. However, the number of pupae formed and flies hatched for SrO-ZTA wear debris treatment groups are almost similar to control groups expect higher treatment concentration (100 µg/mL). Lastly, the current study

* Corresponding author. Laboratory for Material Processing and Engineering, Department of Ceramic Engineering, National Institute of Technology, Rourkela, India.

** Corresponding author. Laboratory of Neural Developmental Biology, Department of Life Science, National Institute of Technology Rourkela, Odisha, 769008, India.

E-mail addresses: mishramo@nitrkl.ac.in (M. Mishra), dsarkar@nitrkl.ac.in (D. Sarkar).

<https://doi.org/10.1016/j.matchemphys.2021.125187>

Received 21 May 2021; Received in revised form 22 August 2021; Accepted 25 August 2021

Available online 26 August 2021

0254-0584/© 2021 Elsevier B.V. All rights reserved.

establishes the non-cytotoxic and non-genotoxic nature of SrO-ZTA wear debris *in-vitro* and *in-vivo*, suggesting promising medical relevance of SrO-ZTA composite.

1. Introduction

Bioceramic based biomaterials contribute efficiently to orthopaedic and medical applications, mostly as implants for damaged/diseased human bone, joints, skeleton, and teeth [1]. In human beings, the most vital articulating or flexible joint is the hip joint which bears the body weight and allows the body with a wide range of motions such as sitting, standing, running, and walking. To date, total hip replacement (THR) surgery is most commonly used treatment of some frequently diagnosed issues like injury, dislocation, osteoarthritis, and inflammatory rheumatoid related diseases in our young generation. However, metallic based implants are frequently used in THR survey. THR therapy is high in demand across the countries as it increases human life expectancy [2]. The femoral head and acetabular socket liner assembly were considered as hip joint bearing. There are mainly four types of bearings i.e., metal-on-metal (MoM), metal-on-polyethylene (MoP), ceramic-on-ceramic (CoC) and ceramic-on-polyethylene (CoP). The mainly used materials for hip prosthesis are ceramic composites, polymers, and metal alloys.

Ceramic's excellent physico-chemical properties attract significant interest in biomedical applications [3]. Alumina, zirconia, and ZTA (Zirconia toughened alumina) composite are considered as ceramic biomaterials. For many years the bioceramic implants remain in close contact with the tissues of the body [4]. Beyond certain years, the performance of the implants was limited owing to the aseptic loosening caused by inflammation in response to the release of wear debris at surface articulation [5]. Numerous *in-vitro/in-vivo* models have been used to substantiate the impact of wear debris on the body. The body immune system treats wear debris as foreign particles and try to eliminate it by phagocytosis just like bacterial infection. Activation of macrophages to internalize the wear debris is marked as the beginning of the osteolysis. But as this wear debris is non-cellular particles, the cellular enzymes fail to effectively degrade it, leading to chronic inflammatory response. Immune response includes activation of cytokines which retards the bone formation process, osteoblast. In humans, wear debris may also activate the inflammasome danger signalling. These particles can also induce apoptosis, inflammatory cytokines production [6]. [7]. Eventually, excessive osteoclast leads to osteolysis and ends up in implant failure [8]. The wear particulates inside the body can cause cytotoxicity, DNA damage, ROS production and cell damage (distorted membrane and enlarged mitochondria) [9–11]. Orthopaedic metal wear debris are also responsible for altered signalling, gene modification and impairment in DNA repair [12,13].

Moreover, these wear debris can accumulate in different body organs and body fluids put human health at risk., Wear debris such as Al and Cr (VI) can initiate microcytic anaemia, while Ni (II) can induce lipid peroxidation [14]. Patients with successful metal-on-metal articulations were identified with reduced CD8⁺ T-cells (circulating lymphocytes) [15]. Humans and experimental models when exposed to debris, may contribute to impairment of renal functions, development of hepatocellular necrosis and tubular necrosis [16,17]. Intoxication and accumulation of wear particulate can elevate the asthma condition, cardiomyopathy and neurodegeneration [18–22]. It has been reported in different animal models that debris comprising Al, Cr (II), Co, Ni and V can impede the production or circulation of sex hormones, alter estrogen signalling and trigger hypothyroidism [22,23]. Retinal degeneration, infertility, hearing impairment, vasculitis and/or urticaria, and dermatitis as a result of wear debris intoxication were also reported [24–28]. Experimental models exposed to wear debris were identified with transgenerational carcinogenesis, teratogenic malformations, and developmental toxicity [29].

With the increasing demand for a novel biomaterial in the medical and orthopaedic fields of bioceramic implants, it has become important to procure the toxicity profile of new and currently used biomaterials [30] to ensure their biocompatibility with the internal environment. Toxicity evaluation of the biomaterials helps to understand the biological interaction of the implants with the body tissues. It helps to determine the stability, longevity, and performance of the implants. The newly developed nanomaterials-based osteoconductive toxicity was recently assessed *in-vitro* and *in-vivo* studies [31,32]. For *in-vitro* analysis, skeletal muscle cells myoblasts or osteoblast cells and for *in-vivo* studies *C. elegans* [33], fruit fly [34], mouse [35], zebrafish [36], and monkey [37] are some preferred models. To date, *Drosophila melanogaster* has been evolved as an excellent model for the study of toxicity of the nanoparticles and nanomaterials [38,39]. *Drosophila* having numerous advantages over other model organisms such as simple and short development cycle, low-cost maintenance, easy handling which makes it a successful model for toxicological studies.

Considering these advantages, the “wear debris” generated during articulating motion of fabricated SrO doped ZTA femoral head and SrO doped ZTA acetabular socket liner in our early research work were collected and used in the current study to check the biological responses of SrO-ZTA wear debris on mouse myoblast cell line C2C12 (*in-vitro*) and *D. melanogaster* (*in-vivo*) model organism.

2. Methodology

2.1. SrO-ZTA wear debris

SrO-ZTA wear debris was generally generated from SrO doped ZTA composite made femoral head's articulating surface and acetabular socket liner. SrO-ZTA wear debris was collected from the assembly of the unpolished femoral head and acetabular socket attached firmly with rotating clockwise under a load of 100 kgf. Further, debris size reduced approximately similar to clinically generated size for *in-vitro* and *in-vivo* experiments [40] (see Fig. 1).

2.2. Characterization of SrO-ZTA wear debris

The SrO-ZTA wear debris was characterized by SEM/EDX, XRD, and Zeta potential to determine the size/element composition, material structure, and surface charge stability, respectively. Firstly, coating of material was done on carbon tape and size/element was analyzed through SEM/EDX (JEOL, JSM-6480LV) at an accelerating voltage of 20 kV. Further, the size of the wear debris was measured using Image J software. X-ray diffraction studies were carried out on a diffractometer ($\lambda_{\text{Cu-K}\alpha}$ = 0.154 nm, Rigaku, Japan) in a scan range between 25° and 55° with the scan speed of 5°/min. To check the Zeta potential of wear debris initially, stock solution of 1 mg/mL was prepared by dispersing SrO-ZTA in distilled water. Thereafter, a homogenous solution was prepared by performing sonication with a pulse of 0.6 for 30 min at 80% amplitude and surface charge stability was measured in Malvern Zeta sizer.

2.3. Cell culture media and reagents

The mouse myoblast cell line C2C12 was procured from National Centre for Cell Science (NCCS), Pune, India to examine the cytocompatibility of the wear debris sample through *in-vitro* analysis. The obtained cell line C2C12 was grown in the Dulbecco's modified Eagle's medium (DMEM, Gibco). The culture medium DMEM was supplemented with 15% fetal bovine serum (FBS, Gibco) and 1% antibiotic-antimycotic (Gibco) for proper cell growth. The cell line C2C12 was grown in

optimum conditions (such as 5% CO₂, 90% humidity, and 37 °C) in a CO₂ incubator (ThermoFisher Scientific, Germany). Subsequently, the cells were trypsinized using 0.05% trypsin-EDTA (Gibco) to maintain a confluent monolayer before performing each *in-vitro* experiment.

2.4. MTT assay

MTT (3-(4, 5-dimethylthiazol-2-yl)-2, 5-diphenyltetrazolium bromide, Sigma Aldrich) assay was performed to check viability and metabolic activity of the cells. The cells were counted and 3×10^3 numbers of cells were seeded in a 96 well plate overnight. Thereafter, wear debris treatment was done at desired concentrations (0.0, 10.0, 20.0, 30.0, 40.0, and 50.0 µg/mL). All the experimental groups were incubated at an optimum condition in the CO₂ incubator for 24, 48, and 72 h with wear debris. The MTT assay was performed following.

2.5. Alexa Fluor 488 phalloidin and DAPI staining

The myoblast cell line C2C12 of 2×10^5 cells/well density was grown on the experimental 6 well culture plate overnight. Treatment of pre-sterilized wear debris was done for 24 and 72 h in an optimized condition. The protocol of Bhaskar et al. was used for Alexa Fluor 488 Phalloidin and DAPI staining of the samples [40].

2.6. Preparation of the wear debris stock solution for in-vivo study

The stock solution (1 mg/mL) of the SrO-ZTA wear debris was prepared by dispersing them in Milli-Q water. Next, the SrO-ZTA solution was sonicated in 80% amplitude with a pulse of 0.6 for 30 min to get a homogenous solution. The sonicated SrO-ZTA solution was mixed in fly food. Then, flies are allowed to feed SrO-ZTA mixed food.

2.7. Fly stock maintenance and experimental setup

The fly stock used in study was *Oregon R* which that we received from Genetics & Developmental Biology Laboratory, Institute of Advanced Research/IIAR Gandhinagar. The flies were reared on the growth medium comprising sucrose, yeast, cornmeal, and Agar type-1. The food vials containing the flies were maintained in a proper environmental condition of light (12 h light: 12 h dark), temperature (23–25 °C), and humidity (70%). The experimental setup contained the control vial (untreated standard food) and four vials of desired concentrations of wear debris (SrO-ZTA) mixed food (10 µg/mL, 25 µg/mL, 50 µg/mL, and/100 µg mL). For the study, 4–5 days old adult virgin female and male flies were selected to set up the control and treatment vials. The complete experimental setup was kept in the optimum fly growth conditions.

2.8. Analysis of larval mid-gut by SEM and EDX

EDX analysis was carried out to check the deposition of SrO-ZTA wear debris inside the larva gut which was fed by flies through food. The third instar larval guts from the experimental food vial were dissected and stored in 4% paraformaldehyde (PFA) at 4 °C overnight. The gut processing was done by following almost similar procedure of Nayak et al. [41] Samples were further coated with gold by a sputter coater (Quorum Technologies, UK) and analyzed under a scanning electron microscope (SEM) (Nova NanoSEM 450). Scanning of midgut was performed on the punctured area inside the midgut to determine the elements that occurred in it through energy-dispersive X-ray spectroscopy (EDX).

2.9. Larva crawling

Larva crawling assay was performed by collecting third instar larvae (5) from each experimental group followed by PBS wash to remove any excess food particles present on the cuticle. Then, the complete procedure was done by following Nayak et al. [41] N.

2.10. Trypan blue

Third instars (5) from each experimental group were collected and were then rinsed in PBS solution (1X) to wash off unwanted food particles from its body surface. Then, the complete procedure was done by following Bag et al. [42].

2.11. Larva Nitro blue tetrazolium (NBT) assay

NBT assay was performed as a determinant of the intracellular reactive oxygen species (ROS). Third instars (15) collected from experimental food vials were properly washed with 1X PBS to remove excess food from the cuticle. Then, the complete procedure was done by following Bag et al. [42].

2.12. Histological stain (DAPI and DCF-DA)

DCFH-DA is an indicator of ROS. 4', 6-diamidino-2-phenylindole (DAPI) is a DNA binding dye, which binds to the minor groove of the double-stranded DNA in the A: T rich region. This dye is often used to visualize the formation of micronuclei or nuclear fragmentation as an indication of DNA damage. For this, third instars (10) collected from each experimental food vials were dissected and fixed in cold (4 °C) PFA overnight. The staining guts with DAPI and DCFDA was carried out by following Nayak et al. and Bag et al. [42,43]. The stained guts were mounted with 20% glycerol to visualize under a fluorescent microscope (Olympus, ISO 800).

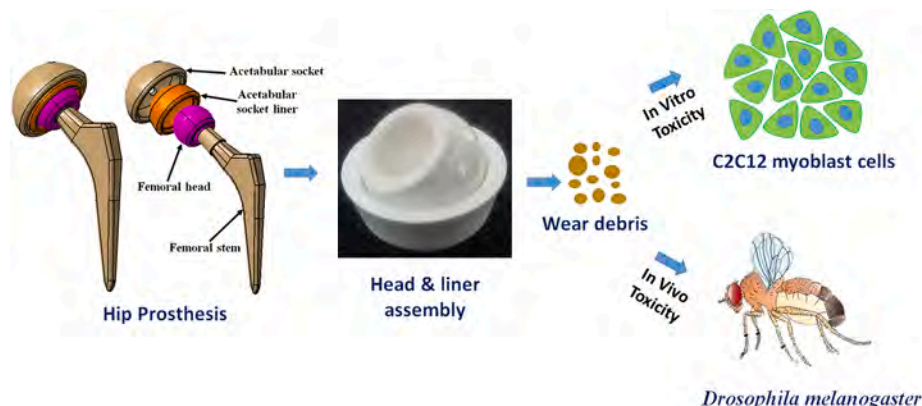


Fig. 1. Schematic representation of biomedical analysis of the present study for the SrO-ZTA generated wear debris.

2.13. Developmental cycle

The fly life cycle is usually of 10–12 days with five stages i.e. larva (first, second and third), pupa and adult stage. Virgin flies of 3–4 days old flies were collected and transferred to each experimental vial in 5 female flies: 3 male flies' ratio. The developmental time points of each stage of all the experimental vials were noted.

2.14. Pupa and hatched fly counting

The number of pupae in each control and treatment vials were counted by marking them each day till the fly hatch. Once the single fly hatched, pupa counting was stopped. The newly hatched flies were transferred from each experimental vials were counted and the graph was plotted [44].

2.15. Adult climbing assay

A measuring cylinder (100 mL) was marked up to 16 cm to perform the assay. Thirty adult flies from each control and treated groups were transferred to the cylinder. Next, steps were done following Bag et al. [42].

2.16. Adult NBT assay

The same steps were followed as that of the larva. The hemolymph was collected by pricking the thorax region of the adult flies. 5 μ L of hemolymph was extracted from 50 flies. Further Nayak et al. protocol was followed to estimate adult ROS [43].

2.17. Adult phenotype

To perform the phenotypic analysis, a stereomicroscope was used to observe 50 flies collected from each vial of different concentrations and imaged. The flies were scanned for any abnormality in bristles, eyes, and wings.

2.18. Statistical analysis

The entire experimental data are represented, from three independent sets of experiments, in terms of mean \pm Standard deviation (SD). The SD represents the error bars. The Student's t-test and two-way ANOVA, statistical tools present in GraphPad Prism 5.0 software was used for the analysis of the experimental data. The values were considered as insignificant (n.s.) when the probability (P) value was >0.05 whereas the values were significant statistically when probability (P) <0.05 and probability (P) <0.01 .

3. Results and discussion

Composite materials are hybrid materials that are derived from the combination of different types of materials depending on their applications. Currently, composites have very extensive industrial usage including medical devices, implants, drug delivery, and bone regeneration. However, it has been observed that the wear debris released from composites may cause severe issues in the recipient. Mainly, the wear debris released from the total joint replacement implants of inorganic materials can cause inflammation in the surrounding tissues, resulting in periprosthetic bone resorption and aseptic loosening [45]. These implant-derived wear debris can aggregate in the various vital organ of the body that can cause severe toxicity [46]. Thus, these wear debris pose a major threat to the survivability and effective application in the patients [47]. A proper analysis of the debris toxic potentiality is needed before the use of the prosthetic implants [48]. Thus, we decided to check whether SrO-ZTA composite based wear debris has any toxic effect in *in-vitro* and *in-vivo* studies.

3.1. Characterization of wear debris

Firstly, it is essential to know the size of a composite based wear debris as the size influences the material reactivity that can affect the toxicity *in-vitro* and *in-vivo*. Veno kononenko et al. have demonstrated the size-dependent genotoxicity of the Zinc oxide (ZnO) in the Madin-Darby canine kidney (MDCK) cells [49]. [50]. The current study found the size of SrO-ZTA based wear debris ranges between 50 and 90 μ m [51, 52]. [53]. The surface morphology and elemental mapping of collected SrO-ZTA wear debris were analyzed by SEM (Nova Nano SEM/FEL) (Fig. 2A). The average size of the wear debris was found to be $73.94 \pm 3.75 \mu$ m. To further determine the distribution of strontium (Sr), aluminium (Al), oxygen (O), zirconia (Zr), EDX analysis was performed at an accelerating voltage of 20 kV (Fig. 2B). We found strong peaks of the different elements present in the SrO-ZTA based wear debris. The EDX analysis result revealed that the collected wear debris was composed of strontium, aluminum, zirconia, and oxygen. XRD analysis was performed to analyze the material structure, which confirms the presence of α -Al₂O₃, t-ZrO₂, and SrAl₁₂O₁₉ phases in wear debris (Fig. 2C). Next, the zeta potential analysis was done to check the biocompatibility of the SrO-ZTA based wear debris. The Zeta potential of SrO-ZTA was -30.5 ± 1.75 mV, which was in acceptable range. Thus, the formulation could be expected to be stable at storage (Fig. 2D).

It has been already established that negatively charged composites are more biocompatible than positive ones [51]. Our result of zeta potential of SrO-ZTA based wear debris was further validated the previous reports that zeta potential of wear debris ranging around ± 30 mV showed more stability and less aggregation [54].

3.2. In-vitro cytocompatibility analysis of SrO-ZTA based wear debris with mouse myoblast cell line C2C12

The amount of wear debris released to the local environment varies with the implant type and composition due to this; our present study is based on the use of desired concentration of the SrO-ZTA based wear debris to mimic the clinical scenario.

3.2.1. Effects of SrO-ZTA on cell survival of mouse myoblast cell line

To check the cytotoxicity of SrO-ZTA wear debris, MTT assay was performed at different concentrations and time intervals in mouse myoblast cell line, C2C12. Treatment results revealed that exposure to SrO-ZTA wear debris did not cause any significant cytotoxicity against the C2C12 cell line at desired treatment concentrations at different time intervals. Indeed, there was no significant difference observed in the proliferation rate of C2C12 at treatment concentrations (10.0, 20.0, 30.0, and 40.0, μ g/mL) of SrO-ZTA wear debris at 24 h. In addition, we found that 50 μ g/mL treatment concentration of SrO-ZTA wear debris significantly promoted the proliferation of C2C12 cell line. Considering the 48 h. SrO-ZTA wear debris treatment results, we found that SrO-ZTA wear debris significantly played a supportive role in the proliferation of C2C12 cell line at all the treated concentrations except 10 μ g/mL treated concentration. Further, at 72 h time point we also observed the proliferation supportive effect of SrO-ZTA wear debris at higher treatment concentrations (30.0, 40.0 and 50.0 μ g/mL) while no significant difference was observed in the proliferation rate of C2C12 cell line at lower treatment concentrations (10.0 and 20.0 μ g/mL). Based on the above findings, we could conclude that exposure of SrO-ZTA wear debris was well tolerated by mouse myoblast cell line C2C12 as well as it supported the proper growth of the C2C12 cell line (Fig. 3). The toxicity of the SrO-ZTA wear debris was first demonstrated in the mouse myoblast cell line, C2C12. Treatment of SrO-ZTA wear debris did not show any toxicity and no growth-promoting effect on C2C12 at 24 h. However, we found a significant increase in cell growth at 48 and 72 h time points without showing any cytotoxicity. Our current findings are also in the agreement with the literature report where ZrO₂-toughened and Al₂O₃-based (ZTA) composite based wear debris had a similar effect on the mouse

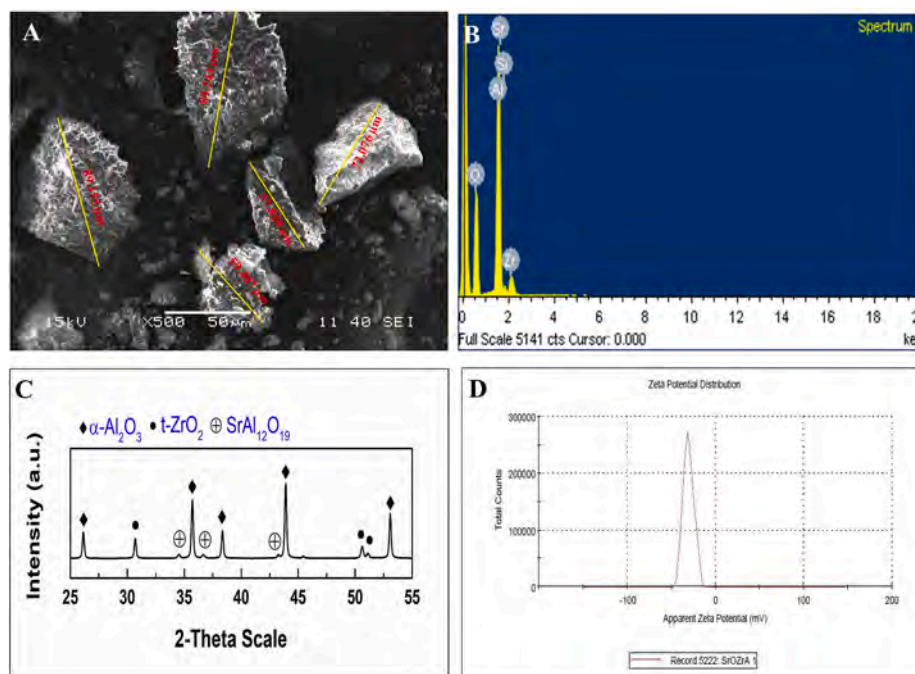


Fig. 2. Characterization of the synthesized SrO-ZTA composite based wear debris. (A) Depicts the size of wear debris using SEM analysis, (B) EDX metal analysis reveals the presence of strontium, aluminium, zirconia, and oxygen, (C) XRD analysis displays the presence of presence of α - Al_2O_3 , t-ZrO_2 , and $\text{SrAl}_{12}\text{O}_{19}$ phases of SrO-ZTA based wear debris, and (D) Surface charge analysis of SrO-ZTA based wear debris based on Zeta potential.

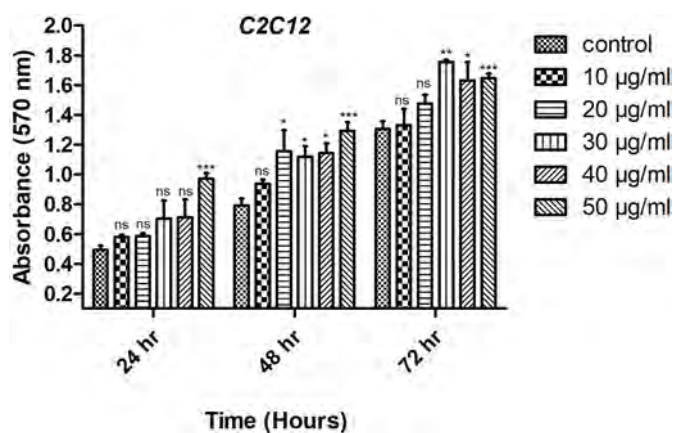


Fig. 3. Cell viability assay showing proliferation supportive role of SrO-ZTA wear debris on mouse myoblast cell line C2C12 at 24, 48, and 72 h treatment time point using MTT.

myoblast cell line C2C12 [55]. On the contrary, the CoCr-ZTA composite based wear debris caused a significant decrease in the growth of *Mus musculus* osteoblast cells growth at 72 h [40].

3.2.2. Cell morphology

Next, the cellular morphology and growth of mouse myoblast cell line C2C12 were analyzed after 72 h incubation with 25 and 50 $\mu\text{g}/\text{mL}$ concentrations of SrO-ZTA wear debris. The fluorescence images showed the cytoskeleton structure i.e., actin filament stained with phalloidin (Fig. 4A–C) and cell nucleus structure stained with DAPI (Fig. 4A'–C'). The cells in the treatment group retained their elongated tubular shape as similar to the control group. Further, the cells were found to be aggregated with the neighbouring cells, and also the cell density was increased, indicating healthy growth of the cells still after exposure of SrO-ZTA wear debris (Fig. 4A'–C''). The fluorescence micrographs exhibited a wide range of cellular growth without any

morphological/cytoskeletal disorganization even after being cultured in presence of SrO-ZTA wear debris till 72 h. Our morphology/cytoskeletal arrangement analysis showed that myoblast cell line C2C12 had distinct cell morphology, define a cytoskeletal organisation, and undeformed nuclear structure still after 72 h incubation with SrO-ZTA wear debris. Our current data is supported by the study on cytotoxicity of ZTA where normal morphology of myoblast cells was observed [55]. There was no sign of cell shrinkage or distorted cell nuclei as seen in cells exposed under metallic nanoparticles [56]. The osteoblast cells seeded with CoCr-ZTA composite wear debris produce a conflict where distorted cell morphology with damaged cells was observed [40]. The cell-cell interaction, enhanced growth, and proliferation of the myoblast cell line on the SrO-ZTA in the present study confirm the cytocompatibility of the SrO-ZTA wear debris. In essence, our study will provide a novel cytocompatible ceramic composite SrO-ZTA and also provides new hope for the patients needing total joint replacement implants.

3.3. In-vivo study of cytotoxicity and genotoxicity effect of SrO-ZTA wear debris on *D. melanogaster*

3.3.1. Analysis of the presence of elements in larval mid-gut

The third instar larva gut was analyzed under the SEM/EDX to confirm the intake of the wear debris by the larva. The larval midgut was collected from each experimental setup and examined under the SEM for elementary deposition (Fig. 5A–E). The EDX data confirmed the higher percentage of aluminium, calcium, and zirconia deposition in the larval gut treated with SrO-ZTA wear debris as compared with the untreated control gut. All the elements of the wear debris were found in small traces inside the larval gut but no traces of strontium were observed in control or treated groups. It is worthy to note that, strontium (Sr) has similarities with calcium (Ca) as it helps in bone formation. From literature, vitamin D induces Sr and Ca inhabitants [57]. The Sr has an important biological effect in bone repair [58] which helps in human bone mineral metabolism. Sr used for bone fracture treatments of postmenopausal women [59], Sr promotes osteogenesis and new bone formation (see Fig. 6). However, there was an increase in the

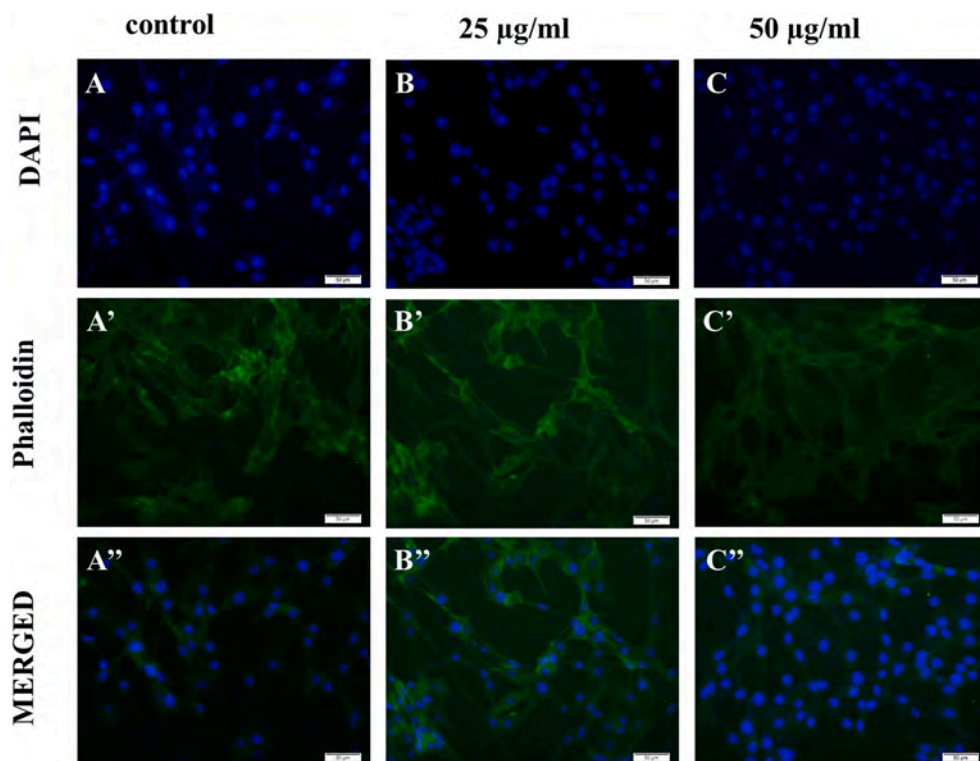


Fig. 4. Effect of SrO-ZTA on the cell morphology of C2C12 cell line after 72 h exposure (A–C) Data showing DAPI stained images of control and SrO-ZTA wear debris treated C2C12 cell line, (A'–C') Alexa flour 488 stained images of control and SrO-ZTA wear debris treated C2C12 cell line after 72 h exposure and, (A''–C'') Merged fluorescence micrographs of DAPI and Phalloidin stained C2C12 cell line.

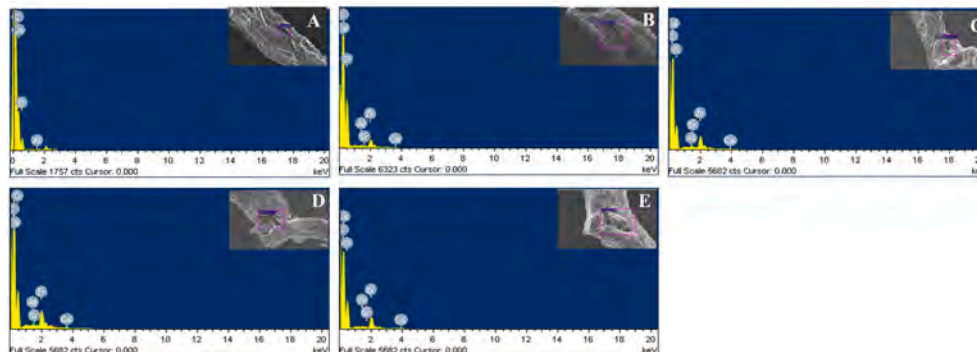


Fig. 5. SEM and EDX metal analysis showing the presence of aluminium, calcium, and zirconia in SrO-ZTA wear debris treated larval gut. (A) Control, (B) 10 µg/mL, (C) 25 µg/mL (D) 50 µg/mL, (E) 100 µg/mL SrO-ZTA wear debris treatments.

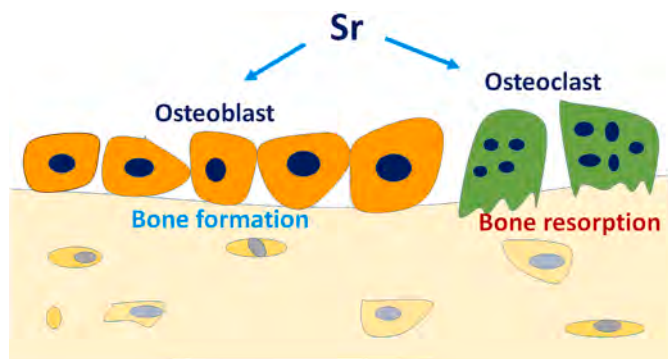


Fig. 6. Effect of strontium on bone formation by osteoblasts and bone resorption by osteoclasts.

concentration of calcium with the increasing concentration of SrO-ZTA based wear debris. Thus, suggesting strontium may have metabolized to calcium, supporting the application of SrO-ZTA as bone implants.

3.3.2. Larva crawling behaviour analysis

Larva crawling behavior is reflected as rhythmic locomotor behavior showed by the third instar larvae. The rhythmic movement is controlled by early developmental neurons in the brain and the neuromuscular junction [60]. The larva crawling assay is a qualitative analysis that tells us about any defect in larval locomotion associated with neuronal damage. The effect of SrO-ZTA wear debris treatment on larva locomotory behavior was observed (Fig. 7A–F). In the control group, larvae took the straight path towards the periphery with a speed of 2.123 ± 0.021 mm/s $N = 3$ and with least number of pause and turn. The speed of larva was slightly increased in 25 µg/mL, 50 µg/mL and 100 µg/mL i.e., 3.400 ± 0.26 mm/s $N = 3$, 2.833 ± 0.14 mm/s $N = 3$ and 2.86 ± 0.12

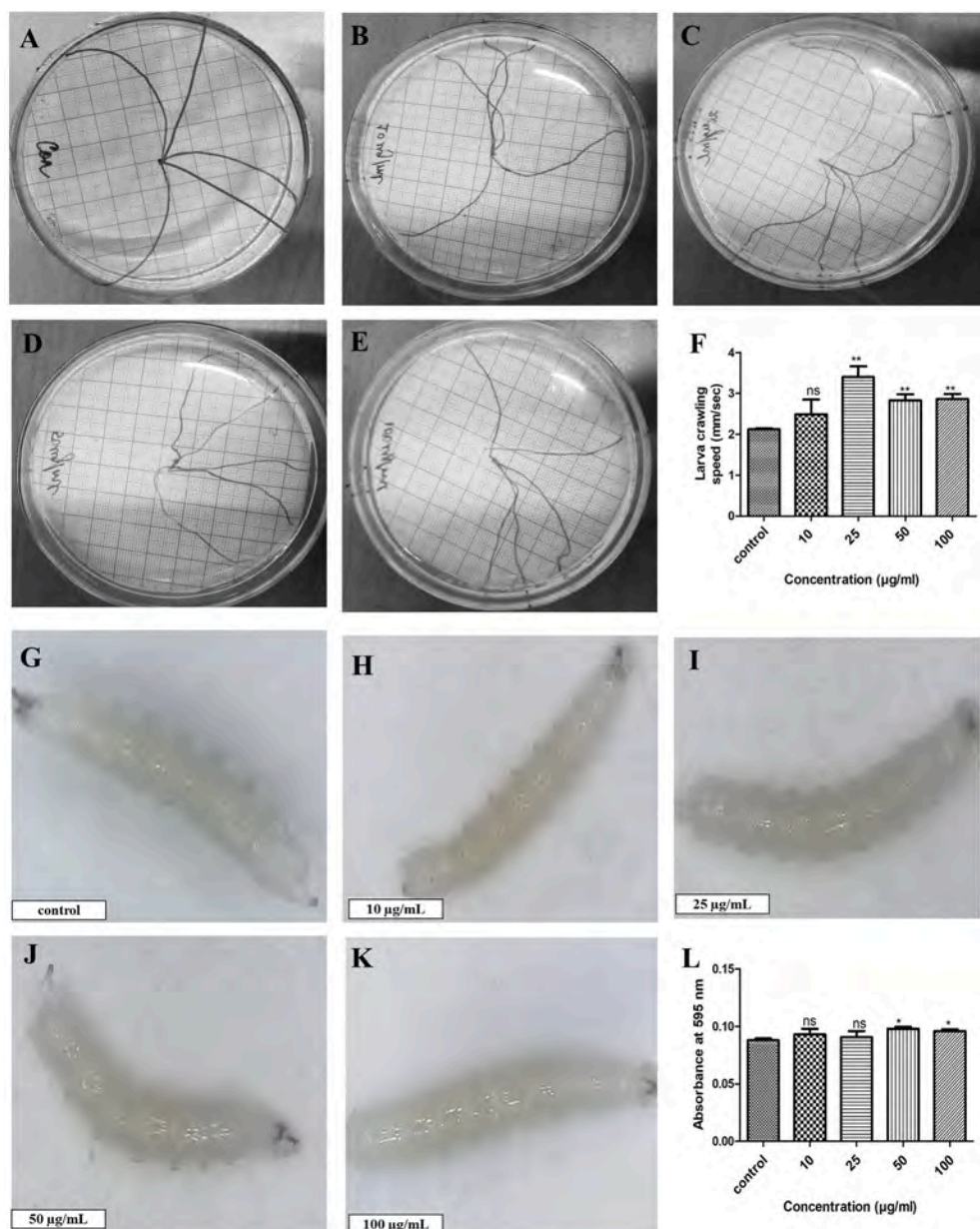


Fig. 7. Effect of SrO-ZTA wear debris on crawling behavior of larva: Data showing walking trails of (A) Control and different SrO-ZTA wear debris treatments (B) 10 µg/mL, (C) 25 µg/mL (D) 50 µg/mL, (E) 100 µg/mL and (F) Increase in larva crawling speed at higher concentration of treatments (25–100 µg/mL) compared to control. Data showing trypan blue stained larva: (G) Control and different SrO-ZTA wear debris treatments (H) 10 µg/mL, (I) 25 µg/mL (J) 50 µg/mL, (K) 100 µg/mL and (L) NBT assay displaying ROS generation in control and SrO-ZTA treated larva. (For interpretation of the references to colour in this figure legend, the reader is referred to the Web version of this article.)

mm/s $N = 3$, respectively. The crawling speed of 10 µg/mL treatment larva was almost similar to that of control i.e., 2.49 ± 0.36 $N = 3$. Earlier studies have reported the neuronal damage in the larva upon ingestion of the nanomaterial as they have disturbed movements with numerous twists and turns [38,61]. In the present study, although the speed of larva in the treatment groups was higher, the larva does not display a defect in the walking trail, which indicates SrO-ZTA wear debris do not induce any toxicity or neuronal cell death.

3.3.3. Trypan blue staining

To examine the toxicity of the composite in our study, SrO-ZTA wear debris was administered to the fly via the oral route. The particles taken up by the fly interacts with the gut cells which have molecules that act as the first line of defense. This interaction may cause gut epithelial cell damage similar to previous reports [62,63]. These damaged cells can be detected by Trypan blue staining of the gut epithelial cells, as it specifically stains the dead cells and is impermeable to the live cells. Trypan blue dye is used to differentiate between live and dead cells, as it only stains the dead and damaged cells, while impermeable to the live cells.

When the voracious feeder third instar larva of treated concentration was stained with trypan blue, they all showed a negative stain as that of the control. Thus, there was no sign of cellular damage due to the ingestion of SrO-ZTA wear debris (Fig. 7G–K). The negative Trypan blue stain suggests SrO-ZTA wear debris do not pose a threat to the gut epithelium.

3.3.4. NBT assay

NBT assay is usually done for the quantification of the number of ROS found in the body. ROS can be detrimental to the organism as it is capable of breaking DNA strands and damaging lipid or protein molecules [64]. NBT assay is usually done for the quantification of the amount of ROS found in the body. We did NBT assay to check the content of the free radicals or the ROS present in the hemolymph of *Drosophila* third instar larvae. The absorbance measured in control and treated samples of varying SrO-ZTA wear debris concentrations suggested that there was no significant oxidative stress of SrO-ZTA wear debris treatments at its lower concentration (10 µg/mL and 25 µg/mL), however higher concentration (50 µg/mL and 100 µg/mL) significantly

induces generation ROS as compared with the control (Fig. 7 L). In our study, a slightly higher concentration of oxidative stress was observed in the higher concentration, which was similar to the earlier study of treatment with gold, silver, and titania nanoparticle [65,66].

3.3.5. Histological staining

DAPI shows the formation of micronuclei or DNA fragmentation and thus is a useful stain to observe DNA damage induced by nanoparticle treatment. DCFDA dye is used to check the intensity of ROS generation. DCFDA dye directly binds to the reactive oxygen molecules and the fluorescent intensity is directly proportional to the amount of ROS. Third instar larvae guts of control and all concentrations of the treated were stained with DAPI and 2, 7-Dichlorofluorescein diacetate (DCFDA) dye to examine the nuclei damage and presence of reactive oxygen molecules, respectively.

It was found that all concentrations of SrO-ZTA wear debris did not cause nuclear damage in treated guts, similar to control guts (Fig. 8A–E). There was an insufficient signal from the different concentrations of SrO-ZTA wear debris treated guts almost similar to control guts, suggesting insignificant production of ROS (Fig. 8 A'–E'). Fig. 8 A''–E'' is the merged image of the larva gut. Positive DAPI stain indicates the apoptotic nuclei in the cells while DCFDA stain intensity provides insight into the status of oxidative stress. Materials inducing cytotoxicity tend to nuclear damage which can be observed as fragmented nuclei upon DAPI staining [67]. In the current study, the treatment samples exhibited negative DAPI stain, with no fragmented nuclei/blebbing and intact round nuclei resembling the control suggesting, no cytotoxic effect of the SrO-ZTA based wear debris in *Drosophila* model. Similarly, the low intensity of the DCFDA stain in all treatment groups suggested that wear debris do not cause oxidative stress to the organisms contrary to the results from other studies [68].

3.3.6. Lifecycle

The lifecycle was checked to analyze the time taken by the eggs to hatch into larva and larva to pupa and finally from pupa hatch into flies.

The lifecycle analysis helps to predict developmental defects caused due to the treatment with SrO-ZTA wear debris. The duration that control flies take to develop from egg to third instar larva was about 72 h, which was same in the treated ones. But in the case of 100 µg/mL concentration, there was an enhancement in larva hatching from an egg. The time taken was approximately around 66 h. The other concentration of the composite wear debris treatment has the same developmental cycle with the control of 10–12 days while the 100 µg/mL treatment causes an advance in life cycle of 7–8 days (Fig. 9). The earlier works were reported the developmental delay due to agglomeration of the Cu, Ca or Ag nanoparticles from treatments [69,70]. However, in the current study, all treatment concentration has a similar developmental cycle as that of the control except for the higher concentration of 100 µg/mL.

3.3.7. Number of pupae formed

The average number of pupae in control was 150.0 ± 0.577 $N = 3$. In treated concentration i.e., 10 µg/mL, 25 µg/mL, 50 µg/mL and 100 µg/mL the average number of pupae formed was found to be 116.0 ± 14.5 $N = 3$, 152.7 ± 1.66 $N = 3$, 127.7 ± 4.33 $N = 3$ and 124.3 ± 3.48 $N = 3$, respectively. At higher concentrations (50 µg/mL and 100 µg/mL) significantly fewer pupas were formed compared to the control (Fig. 10A). The pupae number was recorded to check any developmental defect due to oral intake of SrO-ZTA wear debris which might affect the pupa formation in the flies. A decrease in pupae number at higher concentrations of SrO-ZTA treatment was observed in the current study, which was observed in agreement with the hydroxyapatite particle's treatment [62].

3.3.8. Number of adult flies hatched

The adult flies that were hatched from pupae were counted from all the vials and the number of flies in each treated and control was compared. In treated concentration 10 µg/mL, 25 µg/mL, 50 µg/mL, and 100 µg/mL the average number of flies hatched was found to be 89.67 ± 2.33 $N = 3$, 87.67 ± 1.33 $N = 3$, 81.67 ± 3.84 $N = 3$ and 88.00 ± 1.52 $N = 3$, respectively while in control it was 95.67 ± 0.66 $N = 3$

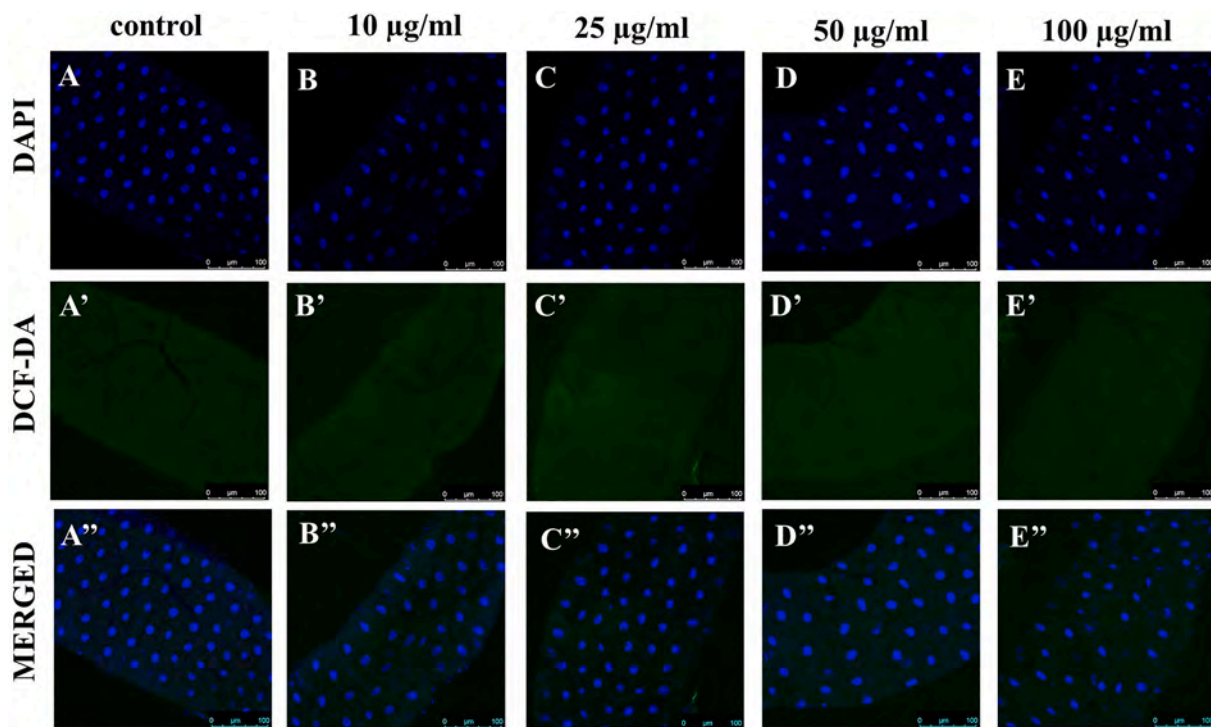


Fig. 8. Effect of SrO-ZTA wear debris on the larval gut nucleus and oxidative stress: (A–E) Data showing DAPI stained images of control and SrO-ZTA wear debris treated larval gut, (A'–E') DCF-DA stained images of control and SrO-ZTA wear debris treated larval gut and, (A''–E'') Merged fluorescence micrographs of DAPI and DCF-DA stained larval gut.

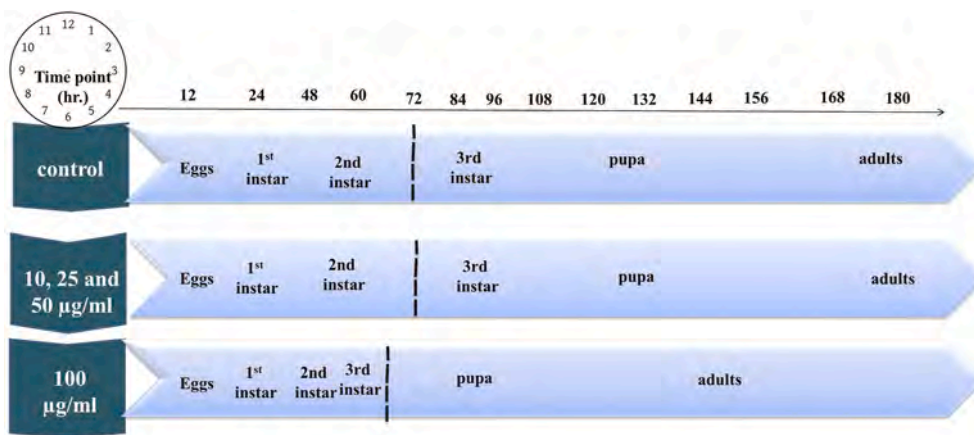


Fig. 9. The developmental cycle analysis of the control and SrO-ZTA wear debris (10 µg/mL, 25 µg/mL, 50 µg/mL and 100 µg/mL) treated flies.

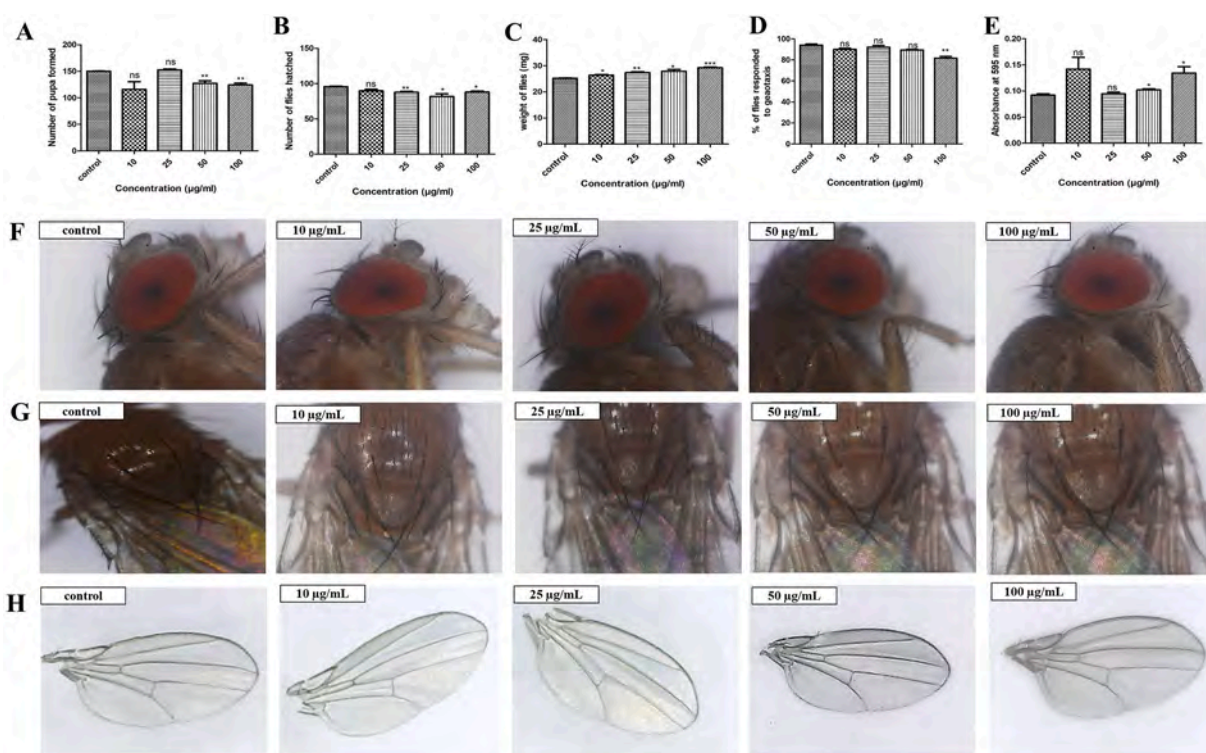


Fig. 10. Effects of SrO-ZTA wear debris treatment on fly physiology, behavior and phenotype. (A) Changes in the number of pupae formation, (B) Number of flies hatched from control and SrO-ZTA wear debris treated pupa, (C) Variation in weight of control and SrO-ZTA wear debris treated flies, (D) Climbing behavior of control and SrO-ZTA wear debris treated flies, (E) NBT assay displaying ROS generation in control and SrO-ZTA wear debris treated adult flies and (F–H) Data showing no phenotypic defects in control and SrO-ZTA wear debris treated flies.

(Fig. 10B). At higher concentrations (25 µg/mL, 50 µg/mL, and 100 µg/mL) less flies were hatched compared with the control. As the pupae number was less compared to the control, in the treatment group, thus less number of flies hatched.

3.3.9. Adult weight

The flyweights were noted and all concentrations feed SrO-ZTA wear debris flies showed an increase in their weight as compared with normal feed control flies (Fig. 10C). It was previously reported that hydroxyapatite and silver nanoparticle treatment significantly caused a decrease in the weight of adult flies [71]. However, in our study, we found a significant increase in adult flies weight in the treatment groups, suggesting SrO-ZTA wear debris do not affect the health of flies.

3.3.10. Adult climbing assay

The adult climbing assay is a behavioral assay that depicts the innate ability of the flies to climb against gravity. The number of flies that climbed past a certain mark was observed. The percentage of flies of the control vial which were able to cross the 16 cm mark within the time limit was $94.00 \pm 1.000\%$ $N = 3$. In treated concentrations, 10 µg/mL, 25 µg/mL, 50 µg/mL, and 100 µg/mL the percentage of flies that were able to climb above 16 cm mark were found to be $90.00 \pm 1.155\%$ $N = 3$, $92.00 \pm 1.732\%$ $N = 3$, $89.33 \pm 0.6667\%$ $N = 3$ and $81.67 \pm 1.667\%$ $N = 3$, respectively (Fig. 10D). The climbing was decreased in 100 µg/mL treated concentration whereas the effect was insignificant in other concentrations of treatment. In the current study, the flies exposed with higher concentrations of wear debris showed positive geotaxis which was in agreement with the previous studies of oral administration of

carbon, gold, and silver nanoparticles [72,73].

3.3.11. Adult NBT assay

We did NBT assay to check the content of the free radicals or the ROS present in the hemolymph of adult flies. The absorbance measured in control and treated samples (varying concentrations of SrO-ZTA wear debris) suggested that there was no significant oxidative stress of wear debris at its lower concentration (10 and 25 µg/mL), however, at its higher concentrations (50 and 100 µg/mL), ROS generation was higher as compared with the control (Fig. 10E). The result of the adult was similar to that of the larva ROS generation. Our data suggested a considerable amount of ROS was produced at higher treatment concentrations of SrO-ZTA wear debris.

3.3.12. Adult phenotype

In the SrO-ZTA wear debris treatment groups, abnormalities related to bristles, eyes, and wings were not observed. However, in adult flies, the external structure of the eye was observed for abnormalities, but no abnormal variations were observed in the wear debris treated flies (Fig. 10F). Additionally, the bristles of the adult flies which respond to sensation were screened for any abnormality, but no abnormality was observed in the wear debris treated flies compared with the control group (Fig. 10G). Adult fly wings were also screened for variation in venation, size of the wings, but no abnormal variations were observed in the wear debris treated flies compared to the control group (Fig. 10H). The eye, antennae and bristle are the sensory organs of the fly that help the flies to perform their daily activities. Defect in any such organ is reflected in the behavior of the fly. In hydroxyapatite nanoparticle treated adult flies, loss of bristles or abnormal bristles were observed, these defects account for defects in the regulatory genes or signalling pathway [74–76]. No such defects were observed after SrO-ZTA wear debris treatment, suggesting it does not induce any defect in regulatory pathways. Similarly to previous findings, venation or wing spots were absent in the flies treated with the SrO-ZTA wear debris. Altogether, the study proves the non-cytotoxicity and non-genotoxicity of SrO-ZTA composite based wear debris *in-vitro* and *in-vivo*.

4. Conclusions

In essence, the present work *in-vitro* analysis demonstrated that SrO-ZTA composite based wear debris enhances cell growth and proliferation, and also has no impact on cellular morphology. The *in-vivo* study in model organism *Drosophila melanogaster* revealed that SrO-ZTA composite based wear debris do not have any cytotoxicity or genotoxicity on the model organism. The non-cytotoxic and non-genotoxic properties of SrO-ZTA composite based wear debris suggest its several biomedical applications, including use as implants. This approach can be adopted to develop other metals, ceramics, polymers, or composites for biomaterial research. The cumulative analysis may use to overcome the limitation of composite use in biomaterial research and explore further material development for clinicians.

CRedit authorship contribution statement

Nibedita Nayak: have performed the *in-vitro* studies, has performed the *in-vivo* studies. **Shaik Akbar Basha:** has developed the wear debris SrO-ZTA, fabricated the component, arranged wear debris particles and completed their characterizations. **Surya Kant Tripathi:** have performed the *in-vitro* studies. **Bijesh K. Biswal:** Supervision. **Monalisa Mishra:** Funding acquisition, Supervision, Funding and supervision. **Debasish Sarkar:** Funding and supervision, Funding acquisition, Supervision.

Declaration of competing interest

The authors declare that they have no known competing financial

interests or personal relationships that could have appeared to influence the work reported in this paper.

Acknowledgments

The current research project is financially supported by the Department of Biotechnology (DBT), Government of India (GOI) (Grant No. BT/PR13466/COE/34/26/2015).

NN is thankful to the DST-INSPIRE for the financial assistance she received for her doctoral work. MM lab is supported by BT/PR21857/NNT/28/1238/2017, SERB/EMR/2017/003054 and Odisha DBT 3325/ST (BIO)-02/2017.

References

- [1] T. Thamaraiselvi, S. Rajeswari, Trends biomater & artif, Organ 18 (2004) 9.
- [2] D. Sarkar, B. Sambhi Reddy, S. Mandal, M. RaviSankar, B. Basu, Uniaxial compaction-based manufacturing strategy and 3D microstructural evaluation of near-net-shaped ZrO₂-toughened Al₂O₃ acetabular socket, Adv. Eng. Mater. 18 (2016) 1634–1644.
- [3] J.M. Cuckler, J. Bearcroft, C.M. Asgian, Femoral Head Technologies to Reduce Polyethylene Wear in Total Hip Arthroplasty, Clinical orthopaedics and related research, 1995, pp. 57–63.
- [4] W. Elshahawy, Advances in ceramics-electric and magnetic ceramics, bioceramics, ceramics and environment, in: Costas Sikalidis. InTech, 2011.
- [5] O.M. Posada, R.J. Tate, M.H. Grant, Effects of CoCr metal wear debris generated from metal-on-metal hip implants and Co ions on human monocyte-like U937, Cells Toxicol. Vitro vol. 29 (2015) 271–280.
- [6] Y. Zhang, M. Yan, A. Yu, H. Mao, J. Zhang, Inhibitory Effects of Beta-Tricalciumphosphate Wear Particles on Osteocytes via Apoptotic Response and Akt Inactivation Toxicology, vol. 297, 2012, pp. 57–67.
- [7] C. Brown, J. Fisher, E. Ingham, Biological effects of clinically relevant wear particles from metal-on-metal hip *Proceedings of the Institution of Mechanical Engineers*, Part H: J. Eng. Med. 220 (2006) 355–369.
- [8] N.J. Hallab, J.J. Jacobs, Biologic Effects of Implant Debris *Bulletin Of the NYU Hospital for Joint Diseases* 67, 2009.
- [9] L. Podleska, M. Weuster, E. Dose, C.A. Kühne, D. Nast-Kolb, S. Ruchholtz, G. Taeger, The impact of nanocolloidal wear-particles on human mononuclear cells *Materialwissenschaft und Werkstofftechnik: entwicklung, Fertigung, Prüfung, Eigenschaften Anwendungen technischer Werkstoffe* 37 (2006) 563–569.
- [10] B. Daley, A. Doherty, B. Fairman, C. Case, Wear debris from hip or knee replacements causes chromosomal damage in human cells in tissue culture *the Journal of bone and joint surgery*, British 86 (2004) 598–606.
- [11] C. Lohmann, Z. Schwartz, G. Köster, U. Jahn, G. Buchhorn, M. MacDougall, D. Casasola, Y. Liu, V. Sylvia, D. Dean, Phagocytosis of wear debris by osteoblasts affects differentiation and local factor production in a manner dependent on particle composition, *Biomaterials* vol. 21 (2000) 551–561.
- [12] A. Witkiewicz-Kucharczyk, W. Bal, Damage of zinc fingers in DNA repair proteins, a novel molecular mechanism in carcinogenesis, *Toxicol. Lett.* 162 (2006) 29–42.
- [13] F. Chen, X. Shi, Intracellular Signal Transduction of Cells in Response to Carcinogenic Metals *Critical Reviews in Oncology/hematology*, vol. 42, 2002, pp. 105–121.
- [14] I. Polyzois, D. Nikolopoulos, I. Michos, E. Patsouris, S. Theocharis, Local and systemic toxicity of nanoscale debris particles in total hip arthroplasty, *J. Appl. Toxicol.* 32 (2012) 255–269.
- [15] A. Hart, T. Hester, K. Sinclair, J. Powell, A. Goodship, L. Pele, N. Fersht, J. Skinner, The association between metal ions from hip resurfacing and reduced T-cell counts *the Journal of bone and joint surgery*, British 88 (2006) 449–454.
- [16] H. Oliveira, T. Santos, J. Ramalho-Santos, M. de Lourdes Pereira, Histopathological effects of hexavalent chromium in mouse kidney, *Bull. Environ. Contam. Toxicol.* 76 (2006) 977–983.
- [17] K. Kametani, T. Nagata, Quantitative elemental analysis on aluminum accumulation by HVTEM-EDX in liver tissues of mice orally administered with aluminum chloride, *Med. Mol. Morphol.* 39 (2006) 97–105.
- [18] P. Nayak, Aluminum: Impacts and Disease *Environmental Research*, vol. 89, 2002, pp. 101–115.
- [19] T. Vlachogianni, K. Fiotakis, S. Lorida, S. Perdicaris, A. Valavanidis, Potential toxicity and safety evaluation of nanomaterials for the respiratory system and lung cancer, *Lung Canc.: Targets Ther.* 4 (2013) 71.
- [20] M. Zywił, J. Brandt, C. Overgaard, A. Cheung, T. Turgeon, K. Syed, Fatal cardiomyopathy after revision total hip replacement for fracture of a ceramic liner *The bone & joint*, Journal 95 (2013) 31–37.
- [21] G. Olivieri, M. Novakovic, E. Savaskan, F. Meier, G. Baysang, M. Brockhaus, F. Müller-Spahn, The effects of β-estradiol on SHSY5Y neuroblastoma cells during heavy metal induced oxidative stress, neurotoxicity and β-amyloid secretion, *Neuroscience* 113 (2002) 849–855.
- [22] V. Sansone, D. Pagani, M. Melato, The effects on bone cells of metal ions released from orthopaedic implants, *Rev. Clin. Cases Mineral Bone Metabolism* 10 (2013) 34.
- [23] P. Darbre, Metalloestrogens: an emerging class of inorganic xenoestrogens with potential to add to the oestrogenic burden of the human breast, *J. Appl. Toxicol. Int. J.* 26 (2006) 191–197.

- [24] Z.-Y. Lu, H. Gong, T. Amemiya, Aluminum chloride induces retinal changes in the rat, *Toxicol. Sci.* 66 (2002) 253–260.
- [25] M.M. Aruldhas, S. Subramanian, P. Sekar, G. Vengatesh, G. Chandrasan, P. Govindarajulu, M. Akbarsha, Chronic chromium exposure-induced changes in testicular histoarchitecture are associated with oxidative stress: study in a non-human primate (*Macaca radiata* Geoffroy), *Hum. Reprod.* vol. 20 (2005) 2801–2813.
- [26] G.M. Keegan, I.D. Learmonth, C. Case, A systematic comparison of the actual, potential, and theoretical health effects of cobalt and chromium exposures from industry and surgical implants, *Crit. Rev. Toxicol.* 38 (2008) 645–674.
- [27] T. Ikeda, K. Takahashi, T. Kabata, D. Sakagoshi, K. Tomita, M. Yamada, Polyneuropathy caused by cobalt–chromium metallosis after total hip replacement, *Muscle Nerve* 42 (2010) 140, 3.
- [28] N. Hallab, K. Merritt, J.J. Jacobs, Metal sensitivity in patients with orthopaedic implants, *JBJS* 83 (2001) 428.
- [29] G. Keegan, I. Learmonth, C. Case, Orthopaedic metals and their potential toxicity in the arthroplasty patient: a review of current knowledge and future strategies *the Journal of bone and joint surgery*, British 89 (2007) 567–573.
- [30] E.A. Koulaouzidou, K. Roussou, K. Sidiropoulos, A. Nikolaidis, I. Kolokuris, A. Tsakalof, C. Tsimipikou, D. Kouretas, Investigation of the chemical profile and cytotoxicity evaluation of organic components eluted from pit and fissure sealants, *Food Chem. Toxicol.* 120 (2018) 536–543.
- [31] S. Chandran, S. Babu, S. VS, H.K. Varma, H.K. John, A *Osteogenic efficacy of strontium hydroxyapatite micro-granules in osteoporotic rat model*, *J. Biomater. Appl.* 31 (2016) 499–509.
- [32] E. Landi, A. Tampieri, G. Celotti, S. Sprio, M. Sandri, G. Logroscino, Sr-substituted Hydroxyapatites for Osteoporotic Bone Replacement *Acta Biomaterialia*, vol. 3, 2007, pp. 961–969.
- [33] X. Yang, A.P. Gondikas, S.M. Marinakos, M. Auffan, J. Liu, H. Hsu-Kim, J.N. Meyer, Mechanism of silver nanoparticle toxicity is dependent on dissolved silver and surface coating in *Caenorhabditis elegans*, *Environ. Sci. Technol.* 46 (2012) 1119–1127.
- [34] S.A. Pappus, M. Mishra, A drosophila Model to Decipher the Toxicity of Nanoparticles Taken through Oral Routes *Cellular And Molecular Toxicology Of Nanoparticles*, 2018, pp. 311–322.
- [35] J. Bahamonde, B. Brenseke, M.Y. Chan, R.D. Kent, P.J. Vikesland, M.R. Prater, Gold nanoparticle toxicity in mice and rats: species differences, *Toxicol. Pathol.* 46 (2018) 431–443.
- [36] C. Chakraborty, A.R. Sharma, G. Sharma, S.-S. Lee, Zebrafish: a complete animal model to enumerate the nanoparticle toxicity, *J. Nanobiotechnol.* 14 (2016) 1–13.
- [37] M. Sedic, J.J. Senn, A. Lynn, M. Laska, M. Smith, S.J. Platz, J. Bolen, S. Hoge, A. Bulychev, E. Jacquinet, Safety evaluation of lipid nanoparticle–formulated modified mRNA in the sprague-dawley rat and cynomolgus monkey, *Veter. Pathol.* 55 (2018) 341–354.
- [38] B.K. Barik, M. Mishra, Nanoparticles as a potential teratogen: a lesson learnt from fruit fly, *Nanotoxicology* 13 (2019) 258–284.
- [39] A. Gautam, C. Gautam, M. Mishra, S. Sahu, R. Nanda, B. Kisan, R.K. Gautam, R. Prakash, K. Sharma, D. Singh, Synthesis, structural, mechanical, and biological properties of HAP-ZrO₂-hBN biocomposites for bone regeneration applications, *Ceram. Int.* (2021). In press.
- [40] N. Bhaskar, D. Sarkar, B. Basu, Probing cytocompatibility, hemocompatibility, and quantitative inflammatory response in *Mus musculus* toward oxide bioceramic wear particulates and a comparison with CoCr, *ACS Biomater. Sci. Eng.* 4 (2018) 3194–3210.
- [41] N. Nayak, M. Mishra, High fat diet induced abnormalities in metabolism, growth, behavior, and circadian clock in *Drosophila melanogaster*, *Life Sci.* 281 (2021) 119758.
- [42] J. Bag, S. Mukherjee, S.K. Ghosh, A. Das, A. Mukherjee, J.K. Sahoo, K.S. Tung, H. Sahoo, M. Mishra, Fe₃O₄ coated guar gum nanoparticles as non-genotoxic materials for biological application, *Int. J. Biol. Macromol.* 165 (2020) 333–345.
- [43] N. Nayak, M. Mishra, Fundamental Approaches to Screen Abnormalities in *Drosophila*, Springer, 2020, pp. 123–134.
- [44] S. Priyadarshini, M. Sahoo, S. Sahu, R. Jayabalan, M. Mishra, An infection of *Enterobacter ludwigii* affects development and causes age-dependent neurodegeneration in *Drosophila melanogaster*, *Invertebr. Neurosci.* 19 (2019) 1–15.
- [45] B. Basu, S. Ghosh, *Biomaterials for Musculoskeletal Regeneration*, Springer, 2017.
- [46] A.K. Madl, M. Liong, M. Kovichich, B.L. Finley, D.J. Paustenbach, G. Oberdörster, Toxicology of wear particles of cobalt-chromium alloy metal-on-metal hip implants Part I: physicochemical properties in patient and simulator studies, *Nanomed. Nanotechnol. Biol. Med.* 11 (2015) 1201–1215.
- [47] A. Paulus, S. Hafelt, V. Jansson, A. Giurea, H. Neuhaus, T. Grupp, S. Utschneider, Histopathological Analysis of Peek Wear Particle Effects on the Synovial Tissue of Patients *BioMed Research International*, 2016, 2016.
- [48] J. Langlois, M. Hamadouche, New animal models of wear-particle osteolysis, *Int. Orthop.* 35 (2011) 245–251.
- [49] V. Kononenko, N. Repar, N. Marušič, B. Drašler, T. Romih, S. Hočevcar, D. Drobne, Comparative in vitro genotoxicity study of ZnO nanoparticles, ZnO macroparticles and ZnCl₂ to MDCK kidney cells: size matters, *Toxicol. Vitro* 40 (2017) 256–263.
- [50] D.J. Gorth, D.M. Rand, T.J. Webster, Silver nanoparticle toxicity in *Drosophila*: size does matter, *Int. J. Nanomed.* 6 (2011) 343.
- [51] X. Li, S.C. Lee, S. Zhang, T. Akasaka, *Biocompatibility and Toxicity of Nanobiomaterials*. Hindawi, 2012.
- [52] L. Zhang, D. Pornpattananangkul, C.-M. Hu, C.-M. Huang, Development of nanoparticles for antimicrobial drug delivery, *Curr. Med. Chem.* 17 (2010) 585–594.
- [53] D.P. Lankveld, A.G. Oomen, P. Krystek, A. Neigh, A. Troost-de Jong, C. Noorlander, J. Van Eijkeren, R. Geertsma, W. De Jong, The kinetics of the tissue distribution of silver nanoparticles of different sizes, *Biomaterials* 31 (2010) 8350–8361.
- [54] Adabi M, Naghibzadeh M, Adabi M, Zarrinfard M A, Esnaashari S S, Seifalian A M, Faridi-Majidi R, Tanimowo Aiyelabegan H and Ghanbari H 2017 *Biocompatibility and nanostructured materials: applications in nanomedicine Artificial cells, Nanomed., Biotechnol.* 45 833-842.
- [55] D. Sarkar, S. Mandal, B. Reddy, N. Bhaskar, D. Sundaresh, B. Basu, ZrO₂-toughened Al₂O₃-based near-net shaped femoral head: unique fabrication approach, 3D Microstruct., Burst Strength Muscle Cell Response Mater. Sci. Eng.: *Chimia* 77 (2017) 1216–1227.
- [56] A. Horikawa, K. Okada, K. Sato, M. Sato, Morphological changes in osteoblastic cells (MC3T3-E1) due to fluid shear stress: cellular damage by prolonged application of fluid shear stress, *Tohoku J. Exp. Med.* 191 (2000) 127–137.
- [57] S.P. Nielsen, The biological role of strontium, *Bone* 35 (2004) 583–588.
- [58] E. Abdullah, A. Idris, A. Saparon, Paper reduction using scs-slm technique in stfbc mimo-odfm, *ARPN J. Eng. Appl. Sci.* 12 (2017) 3218–3221.
- [59] G.M. Blake, I. Fogelman, Strontium ranelate: a novel treatment for postmenopausal osteoporosis: a review of safety and efficacy, *Clin. Interv. Aging* 1 (2006) 367.
- [60] C.D. Nichols, J. Becnel, U.B. Pandey, Methods to Assay *Drosophila* Behavior *Journal Of Visualized Experiments*, JoVE, 2012.
- [61] P.K. Mishra, A. Ekielski, S. Mukherjee, S. Sahu, S. Chowdhury, M. Mishra, S. Talegaonkar, L. Siddiqui, H. Mishra, Wood-based cellulose nanofibrils: haemocompatibility and impact on the development and behaviour of *Drosophila melanogaster*, *Biomolecules* 9 (2019) 363.
- [62] S.A. Pappus, B. Ekka, S. Sahu, D. Sabat, P. Dash, M. Mishra, A toxicity assessment of hydroxyapatite nanoparticles on development and behaviour of *Drosophila melanogaster*, *J. Nanoparticle Res.* 19 (2017) 136.
- [63] M. Mishra, D. Sabat, B. Ekka, S. Sahu, P. Unnikannan, P. Dash, Oral intake of zirconia nanoparticle alters neuronal development and behaviour of *Drosophila melanogaster*, *J. Nanoparticle Res.* 19 (2017) 282.
- [64] E. Zhu, Y. Li, C.-Y. Chiu, X. Huang, M. Li, Z. Zhao, Y. Liu, X. Duan, Y. Huang, In situ development of highly concave and composition-confined PtNi octahedra with high oxygen reduction reaction activity and durability, *Nano Research* 9 (2016) 149–157.
- [65] E. Demir, G. Vales, B. Kaya, A. Creus, R. Marcos, Genotoxic analysis of silver nanoparticles in *Drosophila*, *Nanotoxicology* 5 (2011) 417–424.
- [66] R. Posgai, C.B. Cipolla-McCulloch, K.R. Murphy, S.M. Hussain, J.J. Rowe, M. G. Nielsen, Differential toxicity of silver and titanium dioxide nanoparticles on *Drosophila melanogaster* development, reproductive effort, and viability: size, coatings and antioxidants matter, *Chemosphere* 85 (2011) 34–42.
- [67] A.S. Anand, D.N. Prasad, S.B. Singh, E. Kohli, Chronic exposure of zinc oxide nanoparticles causes deviant phenotype in *Drosophila melanogaster*, *J. Hazard Mater.* 327 (2017) 180–186.
- [68] E. Asadpour, H.R. Sadeghnia, A. Ghorbani, M. Sedaghat, M.T. Boroushaki, Oxidative stress-mediated cytotoxicity of zirconia nanoparticles on PC12 and N2a cells, *J. Nanoparticle Res.* 18 (2016) 14.
- [69] H. Chen, B. Wang, W. Feng, W. Du, H. Ouyang, Z. Chai, X. Bi, Oral magnetite nanoparticles disturb the development of *Drosophila melanogaster* from oogenesis to adult emergence, *Nanotoxicology* 9 (2015) 302–312.
- [70] A. Panacek, R. Prucek, D. Safarova, M. Dittrich, J. Richtrova, K. Benickova, R. Zboril, L. Kvitek, Acute and chronic toxicity effects of silver nanoparticles (NPs) on *Drosophila melanogaster*, *Environ. Sci. Technol.* 45 (2011) 4974–4979.
- [71] A. Raj, P. Shah, N. Agrawal, Sedentary Behavior and Altered Metabolic Activity by AgNPs Ingestion in *Drosophila melanogaster* *Scientific Reports*, vol. 7, 2017, pp. 1–10.
- [72] X. Liu, D. Vinson, D. Abt, R.H. Hurt, D.M. Rand, Differential toxicity of carbon nanomaterials in *Drosophila*: larval dietary uptake is benign, but adult exposure causes locomotor impairment and mortality, *Environ. Sci. Technol.* 43 (2009) 6357–6363.
- [73] S.C.S. Key, D. Reaves, F. Turner, J.J. Bang, Impacts of silver nanoparticle ingestion on pigmentation and developmental progression in *Drosophila* *Atlas*, *J. Biol.* 1 (2017) 52–61.
- [74] M.T. Peña-Rangel, I. Rodriguez, J.R. Riesgo-Escovar, A Misexpression Study Examining Dorsal Thorax Formation in *Drosophila melanogaster* *Genetics*, vol. 160, 2002, pp. 1035–1050.
- [75] J. Culi, E. Martín-Blanco, J. Modolell, The EGF Receptor and N Signaling Pathways Act Antagonistically in *Drosophila* Mesothorax Bristle Patterning *Development*, vol. 128, 2001, pp. 299–308.
- [76] D. Furman, T. Bukharina, Genetic Control of Bristle Pattern Formation in *Drosophila melanogaster*, vol. 417, Springer, 2007, pp. 484–486.